Remote control: the cancer cell-intrinsic mechanisms that dictate systemic inflammation and anti-tumor immunity

Wellenstein, M.D.

Proteomic characterization of neutrophils in metastatic breast cancer reveals tissue- and maturation state-specific phenotypes

Max D. Wellenstein[1], Seth B. Coffelt[1, 2], Onno B. Bleijerveld[3], Hannah Garner[1], Cheei-Sing Hau[1], Kim Vrijland[1], Maarten Altelaar[3, 4], Karin E. de Visser[1, 5], *

Manuscript in preparation

Affiliations

[1] Division of Tumor Biology & Immunology, Oncode Institute, Netherlands Cancer Institute, Amsterdam, The Netherlands; [2] Present address: Institute of Cancer Sciences, University of Glasgow, Glasgow, UK; Cancer Research UK Beatson Institute, Glasgow, UK; [3] Proteomics Facility, Netherlands Cancer Institute, Amsterdam, The Netherlands; [4] Biomolecular Mass Spectrometry and Proteomics, Utrecht Institute for Pharmaceutical Sciences, Utrecht University, Utrecht, The Netherlands; [5] Department of Immunohematology and Blood Transfusion, Leiden University Medical Centre, Leiden, Netherlands.

* Corresponding author

Abstract

The immune system plays an essential role in virtually all aspects of cancer. While some immune cell types are able to elicit anti-tumor responses, others can aid cancer development and metastasis. Neutrophils have been implicated in promoting cancer progression. Emerging insights suggest that cancer-induced neutrophils can acquire a diverse set of activation states depending on tumor type, disease stage and tissue of residence. However, the phenotypic diversity of neutrophils in breast cancer remains elusive and the functional impact of this diversity on the development of cancer is largely unknown. Using proteomic analysis on neutrophils from a genetically engineered mouse model for breast cancer, we here show that anatomical locations shape neutrophil phenotypes under homeostatic conditions and that tumor-derived signals largely override this tissue-specific activation state. We further demonstrate that a subset of neutrophils in mammary tumor-bearing mice expresses the stem cell marker cKIT and that this subset represents a less differentiated cell with distinct protein expression compared to cKIT$^-$ neutrophils. Finally, we show that antibody-mediated targeting of cKIT reduces mammary tumor growth and metastasis formation via as of yet unknown mechanisms. Future studies may reveal the functional relevance of these tissue-specific and subset-specific phenotypes to neutrophil biology in metastatic breast cancer.

Introduction

Neutrophils play a key role in the defense against infections and in wound healing responses. These anti-pathogenic functions of neutrophils are often hijacked and manipulated in tumor-bearing hosts, resulting in a spectrum of outcomes ranging from tumor-promoting to tumor-limiting[1,2]. On one hand, their vast arsenal of proteases, reactive oxygen and nitrogen molecules and other granular effector proteins, used to neutralize pathogens during infection, can induce anti-tumorigenic effects in pre-clinical cancer models[3-6]. Conversely, under the chronic inflammatory conditions that are often induced by tumors, neutrophils can display tumor-promoting and immune-modulatory effects. This includes stimulation of angiogenesis, promotion of cancer cell migration and survival, as well as suppression of cytotoxic immune cells[7-18]. As such, neutrophils exert important functions in the initiation, growth and progression of a large variety of tumor types[1]. In line with these pre-clinical findings, systemic neutrophilia in cancer patients has been consistently associated with poor disease outcome across solid cancer types[19]. However, the association between intratumoral neutrophil levels and cancer outcome is less clear, as both adverse and favorable associations between intratumoral neutrophil levels and disease outcome have been described[20-23]. These (pre-) clinical insights regarding intratumoral and systemic neutrophilia highlight the diverse phenotypes that neutrophils can acquire in cancer. Because of their important role in tumor biology, targeting neutrophils for therapeutic purposes has gained attention over recent years. However, to be able to potentiate their anti-cancer effects and to negate their tumor-promoting characteristics, it is crucial to gain a deeper understanding of what underlies the diverse phenotypes of neutrophils.

Neutrophils were once thought to be a homogeneous cell type with limited diversity in effector phenotypes, mainly due to their short lifespan and terminal differentiation state when they leave the bone marrow. However, recent evidence demonstrates highly specialized phenotypes depending on the anatomical location in which these cells reside, even under homeostatic conditions[24]. Examination of the fate of neutrophils as they leave the circulation and enter tissues has revealed that these cells have a diverse set of regulatory functions under non-pathogenic conditions, which are both organ-specific and occur in an oscillating fashion depending on circadian rhythms[24,25]. Moreover, comparing myeloid cells from different non-perturbed tissues revealed that neutrophils have organ-specific expression of cell surface molecules, hinting towards phenotypic diversity depending on tissue of residence[26]. Under non-homeostatic conditions, such as cancer, these organ- and time-dependent phenotypes also alter neutrophil effector function[24,25,27]. For example, seeding of intravenously injected B16F1 melanoma cell lines in lungs was counteracted by neutrophils only at given times during the day[24]. In another report using subcutaneously implanted B16F1 melanoma cell lines, neutrophils in tumors and tumor-draining lymph nodes, but not in spleen, blood or bone marrow, exhibited a tumor-promoting immunosuppressive phenotype, characterized among others by expression of genes encoding PD-L1 and iNOS[27]. This suggests that although neutrophils expand systemically, they adapt their phenotypes to specific environments. This is also reflected by a comparison of transcriptome profiles of intratumoral neutrophils from different subcutaneously inoculated cell line models, which demonstrated that neutrophils that reside in B16 melanomas, 4T1 breast tumors or Her2 breast tumors are transcriptionally distinct[28]. Because all tumors were inoculated subcutaneously, this suggests that these phenotypes are dictated by differences between the tumors, such as tumor (sub)type or oncogenic drivers expressed by these tumors. These studies demonstrate a previously

underappreciated complexity and plasticity in neutrophil phenotypes depending on anatomical location, cancer type and other unknown elements, which requires further elucidation.

Another aspect of neutrophil diversity that remains underexplored is the functional significance of their differentiation state or maturity[29]. Under homeostatic conditions, neutrophils only leave the bone marrow fully differentiated, with a segmented nuclear morphology[30]. When demand for neutrophils is high due to pathogenic infection, hematopoiesis becomes myeloid-biased to facilitate generation and release of large numbers of neutrophils in a process called emergency granulopoiesis[31]. Due to this high pressure on neutrophil release from the bone marrow, mediated by chemokines such as granulocyte colony stimulating factor (G-CSF), neutrophils with an immature phenotype –as evidenced by ring-shaped or banded nuclear morphology[30]– egress from the bone marrow into the periphery in this process[31]. These immature neutrophils have also been observed in the periphery of mouse tumor models and cancer patients[15,29,32-36]. It is therefore hypothesized that tumor-induced factors, including G-CSF, induce a state of emergency granulopoiesis and thus instruct the bone marrow to release not fully differentiated, immature, neutrophil progenitor cells[37].

Immature neutrophils have been reported to functionally deviate from mature neutrophils in chemokine receptor expression, migratory function, reactive oxygen and nitrogen species (ROS/RNS) production and granular content[38]. As neutrophils mature, their cell size and granular content increases, which results in the observation that mature neutrophils have high cellular density properties (high-density neutrophils (HDN)) and immature neutrophils have lower density (low-density neutrophils (LDN))[32]. It is of note that LDN represent a heterogeneous population in terms of maturity, with approximately 60% of cells showing non-segmented nuclei[32]. Also, neutrophil density decreases upon activation[39], likely as a result of degranulation, indicating that the link between neutrophil maturity and density is not clear-cut. Regardless, HDN and LDN differ substantially in phagocytosis and immunosuppressive capacities, as well as ROS production[32]. Mature and immature neutrophils can also be distinguished by expression of cell surface proteins, although a universally applicable set of markers remains to be established. For example, neutrophil progenitor cells in bone marrow can be identified by expression of the tyrosine kinase receptor cKIT[38,40,41]. We and others have shown that peripheral neutrophils in tumor-bearing hosts express this receptor as well[15,36,42]. Characterization of immature neutrophils based on cKIT expression has demonstrated deviating functions from mature cKIT$^-$ neutrophils, including pro-tumorigenic properties[41]. Expression of the cKIT receptor can therefore be used to distinguish tumor-induced immature neutrophils from mature neutrophils and to study the functional role of these different maturation states.

Because the impact of anatomical location and maturation state on neutrophil phenotypes in breast cancer is poorly described, we set out to characterize neutrophils from various organs in a genetically engineered mouse model for metastatic breast cancer. By analyzing the proteome of neutrophils in circulation and lungs, we found tissue-specific protein expression profiles in wild-type (WT) mice, which are largely lost in tumor-bearing hosts. We further show that mammary tumor-induced cKIT$^+$ and cKIT$^-$ neutrophils also have variations in their proteome, depending on the anatomical location in which they reside. Lastly, we show that targeting cKIT *in vivo* impacts tumor progression and metastasis. This work sheds light on organ-specific and maturation-state-specific neutrophil phenotypes that could potentially be important for breast cancer development and therefore require further

investigations.

Results

Neutrophils expand systemically in the K14-cre;Cdh1$^{F/F}$;Trp53$^{F/F}$ mouse model for metastatic breast cancer

Given that systemic neutrophilia is associated with poor prognosis in breast cancer[43] and neutrophils can impact the pre-metastatic niche and formation of metastatic lesions[1], we sought to characterize these cells in metastatic breast cancer. To this end, we utilized the *K14-cre;Cdh1$^{F/F}$;Trp53$^{F/F}$* (KEP) mouse model for invasive lobular carcinoma[44]. We orthotopically transplanted KEP tumor fragments into WT syngeneic mice and assessed systemic neutrophil expansion. We observed a striking increase in frequency of these cells in circulation, lungs and spleen of KEP tumor-bearing mice compared to WT control mice (**Fig. 8.1a**). As we have reported previously, neutrophils can promote metastasis of KEP tumors by adapting immunosuppressive functions, mainly via the production of nitric oxide (NO), thus limiting anti-tumor T cell responses[15]. To determine whether expression of the enzyme responsible for producing NO (iNOS) differs between neutrophils from circulation, lungs or spleen, we isolated these cells from these different organs and assessed *Nos2* expression.

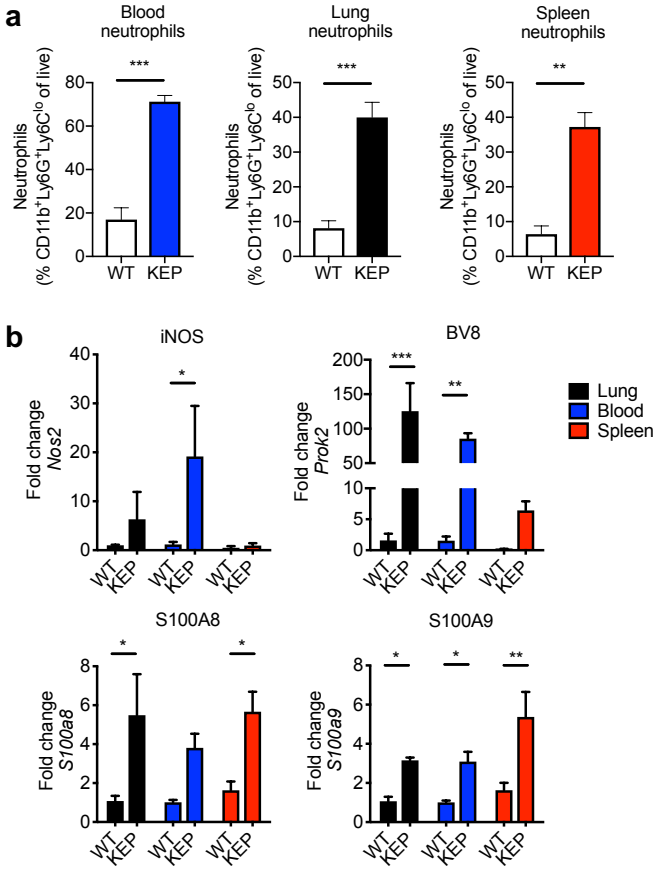

Figure 8.1. Mammary tumors induce systemic neutrophilia and expression of metastasis-associated genes. a. Frequency of neutrophils (% $CD11b^+$ $Ly6G^+Ly6C^{low}$ of total live cells) in blood (blue), lungs (black) and spleen (red) of mice bearing orthotopically transplanted KEP tumors (100 mm^2) or WT control mice, as determined by flow cytometry (n=5–8 biological replicates/ group). **b.** RT-qPCR analysis of neutrophils isolated from blood (blue), lungs (black) and spleen (red) from orthotopically transplanted KEP tumor-bearing and WT mice for expression of *Nos2, Prok2, S100a8* and *S100a9* (n=2–3 biological replicates/group, performed in technical duplicate). All data are ± S.E.M.; * P < 0.05, ** P < 0.01, *** P < 0.001, as determined by two-sided Mann-Whitney test (**a**) or Fisher's LSD test (**b**).

When comparing neutrophils from KEP or WT mice, we observed that tumor-induced *Nos2* upregulation is most significant in circulating neutrophils, while in lungs only a trend of increased expression is observed and expression is unaltered in spleen neutrophils (**Fig. 8.1b**). Assessment of other genes implicated in the pro-metastatic phenotype of neutrophils, *Prok2*, *S100a8* and *S100a9* [11,15,45] (encoding BV8, S100A8 and S100A9, respectively), further revealed organ-specific expression patterns. While *Prok2* was significantly upregulated in neutrophils from lungs and circulation, *S100a8* showed upregulation in lungs and spleen, and *S100a9* was increased in expression in all three organs of KEP tumor-bearing mice compared to WT controls (**Fig. 8.1b**). These data indicate that KEP mammary tumors can induce neutrophil expansion throughout the body and these cells can adapt tissue-specific expression profiles of genes that have been implicated in promotion of metastasis.

Neutrophils exhibit tissue-specific proteome profiles in wild-type mice that are largely revoked in mammary tumor-bearing hosts

The tissue-specific gene expression patterns we observed in neutrophils may have implications for how these cells function in different organs of the tumor-bearing host. This notion prompted us to further characterize the molecular changes in neutrophils that reside in different anatomical locations. To this end, we isolated neutrophils from circulation and lungs of transgenic KEP mice and age-matched WT controls and analyzed their proteome using liquid-chromatography-coupled tandem mass spectrometry (LC-MS/MS). Unsupervised clustering of the differentially expressed proteins revealed that neutrophils in WT mice deviate in their proteomic profile depending on whether they are circulating or present in the lungs (**Fig. 8.2a, b**). Moreover, notably changes were observed when comparing neutrophils from KEP and WT mice (**Fig. 8.2a, b**). Strikingly however, there was a large degree over overlap between neutrophils from KEP mice, regardless of their anatomical location (**Fig. 8.2a, b**), indicating that the tissue-specific changes observed in WT animals were largely lost in neutrophils from tumor-bearing KEP mice.

Upon detailed comparison of circulating neutrophils from KEP and WT mice, we observed marked changes in protein expression (**Fig. 8.2c**). In KEP-induced neutrophils, we observed a significant decreased abundance of proteins related to metabolism and chemotaxis of neutrophils, such as ALOX12 and ALOX12L (also known as ALOX15)[46-48]. Other proteins decreased in circulating neutrophils from KEP mice included ITGA2b (also known as CD41) and Platelet glycoprotein V (**Fig. 8.2c**), which may indicate altered

Figure 8.2. Neutrophils show tissue-specific proteomic profiles that are largely overruled in tumor-bearing mice. a. Heatmap depicting the differentially expressed proteins ($P < 0.05$) in blood and lung neutrophils of WT and KEP mice**. b.** Principal component analysis (PCA) of blood and lung neutrophils of WT and KEP mice. **c.** Volcano plot of differentially expressed proteins comparing circulating neutrophils from KEP tumor-bearing mice and WT controls as determined by LC-MS/MS. **d.** Volcano plot of differentially expressed proteins comparing lung neutrophils from KEP tumor-bearing mice and WT controls as determined by LC-MS/MS. **e.** Volcano plot of differentially expressed proteins comparing neutrophils from lungs with circulating neutrophils in WT mice. **f.** Volcano plot of differentially expressed proteins comparing neutrophils from lungs with circulating neutrophils in KEP tumor-bearing mice. Horizontal red lines in volcano plots indicate $P < 0.05$ and vertical green lines indicate a $\log_2$-transformed fold change in expression > 1. All analyses contain 4 biological replicates per group. For KEP groups, transgenic KEP mice were used and neutrophils were isolated at 100 mm^2 tumor size. For WT groups, 2 mice were pooled per biological replicate to obtain sufficient protein. Lung and blood neutrophils were taken from the same mice for each biological replicate.

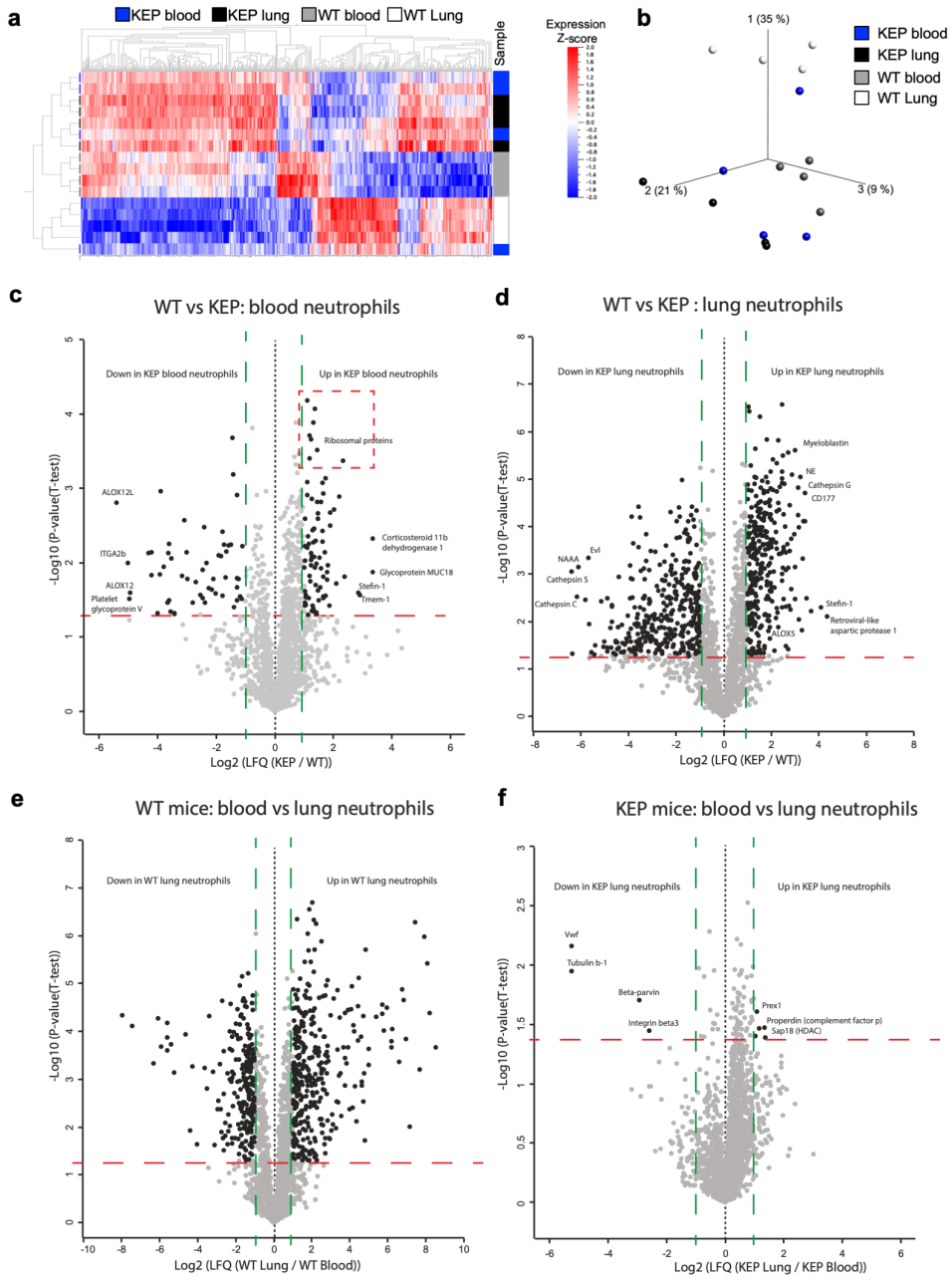

interactions with platelets[49]. We observed an increase in proteins involved in regulation of inflammatory processes in neutrophils from KEP mice, such as MUC18 and Corticosteroid dehydrogenase 1 [50,51]. In addition, we observed a striking enrichment of ribosomal proteins in circulating neutrophils from KEP mice (**Fig. 8.2c**), which may suggest a tumor-induced

activation of translation in these cells. Others have shown that protein translation in 66cl4 mammary tumor cell line-induced neutrophils was key in survival and pro-metastatic function of mammary tumor-induced neutrophils[52]. Gene ontology (GO) analysis revealed an increase of rRNA and mRNA binding activity in circulating neutrophils from KEP mice compared to WT controls, and a decrease in processes such as Arachidonate 15-lipoxygenase, antioxidant and peroxidase activity (**Supplemental Fig. 8.1a**). These data reveal that KEP tumors induce proteomic changes in circulating neutrophils related to metabolism, effector function and translation.

Next, we analyzed neutrophils that reside in lungs of KEP tumor-bearing mice or WT controls (**Fig. 8.2d, Supplemental Fig. 8.1b**). In KEP neutrophils from lungs, we observed an increase in expression of effector proteins such as neutrophil elastase (NE), Myeloblastin and Cathepsin G. Additionally, CD177 was increased in lung neutrophils from KEP mice (**Fig. 8.2d**). CD177 is expressed in neutrophil progenitors and mature neutrophils[53]. It also marks an activated state in inflammatory diseases[54] and is required for transmigration and survival of neutrophils[55]. ALOX5 was upregulated in lung neutrophils from KEP mice, which has been reported to endow neutrophils with pro-metastatic functions[16]. Interestingly, we also saw Cathepsin S decreased, which is a protease involved in peptide processing for presentation of antigen on major histocompatibility complex (MHC)-II[56]. Although Cathepsin S and antigen presentation have not been linked in neutrophils per se, antigen presentation by neutrophils has been implicated in tumor-antagonizing functions in early-stage lung cancer[57]. In both lung and blood KEP neutrophils, we observed an increased expression of Steffin-1 (or Steffin A1) (**Fig. 8.2c, d**), which also functions in protein processing by among others inhibition of Cathepsin S[58], potentially linking to its decreased protein levels. Whether these changes alter neutrophil function in lungs remains to be evaluated.

We then examined the changes neutrophil phenotypes depending on anatomical location. To this end, we compared lung with circulating neutrophils within WT mice, or within KEP tumor-bearing mice. As evidenced from the clustering and principal component

Figure 8.3. Neutrophils expressing cKIT expand systemically in mammary tumor-bearing mice and show minor phenotypical changes compared to cKIT$^-$ neutrophils. a. Frequency of cKIT-expressing neutrophils (% of cKIT$^+$ of total live CD11b$^+$Ly6G$^+$Ly6C^{low} cells) in blood (blue), lungs (black) and spleen (red) of mice bearing orthotopically transplanted KEP tumors (100 mm^2) or WT control mice, as determined by flow cytometry (n=4–8 biological replicates/group). **b.** Representative images of circulating neutrophils from transgenic KEP mice with 100 mm^2 tumors as visualized by ImageStream analysis. Nuclear morphology was assessed by DRAQ5 cell-permeable nuclear dye. **c.** Quantification of nuclear morphology based on ImageStream analysis of circulating neutrophils from transgenic KEP mice with 100 mm^2 tumors. Data were normalized to cKIT$^-$ neutrophils of WT mice (n=3 biological replicates/group). **d.** RT-qPCR analysis of cKIT$^+$ and cKIT$^-$ neutrophils isolated from blood of orthotopically transplanted KEP tumor-bearing and WT mice for expression of *Nos2, Prok2, S100a8* and *S100a9* (n=3–7 biological replicates/group, performed in technical duplicate). **e.** NO levels in neutrophils as determined by DAF-FM diacetate fluorescent probe in cKIT$^-$ neutrophils from WT blood and cKIT$^+$ and cKIT$^-$ neutrophils from blood of transgenic KEP mice with 100 mm^2 tumors. Where indicated, cells were treated *ex vivo* with iNOS inhibitor L-NMMA (7–8 biological replicates/group). **f.** Volcano plot of differentially expressed proteins comparing cKIT$^+$ and cKIT$^-$ neutrophils from blood (left) or lungs (middle) from KEP tumor-bearing mice or comparing cKIT$^+$ neutrophils from lungs with those from blood (right). Horizontal red lines in volcano plots indicate $P < 0.05$ and vertical green lines indicate a $\log_2$-transformed fold change in expression > 1. All analyses contain 4 biological replicates per group. For KEP neutrophil mass spectrometry, transgenic KEP mice were used and neutrophils were isolated at 100 mm^2 tumor size. All data are ± S.E.M.; * $P < 0.05$, ** $P < 0.01$, as determined by two-sided Mann-Whitney test (**a**), c^2-test (**c**), Fisher's LSD test (**d**), or one-way ANOVA (**e**).

analysis (**Fig. 8.2a, b**), we observed marked changes in neutrophil proteome in WT animals depending on the anatomical location in which they reside (**Fig. 8.2e**). Gene ontology analysis revealed that circulating neutrophils from WT mice are mainly enriched for cytotoxic effector functions compared to lung neutrophils, and that lung neutrophils are enriched for metabolic pathways compared to those in circulation (**Supplemental Fig. 8.1c**). One such metabolic pathway pertaining to fatty acids has recently been linked to neutrophil-mediated immunosuppression[59]. As noted above, these organ-specific differences largely disappear in tumor-bearing mice (**Fig. 8.2f**). Together, these data show that under non-cancer conditions, neutrophils adapt a tissue-specific proteome, most likely as a result of the organ-specific signaling environments that affect functionality of these cells. In tumor-bearing mice, however, neutrophils adapt a tumor-induced phenotype that is similar in circulation and (pre-) metastatic lungs, suggesting that the tumor-derived signals largely override the tissue-specific signals.

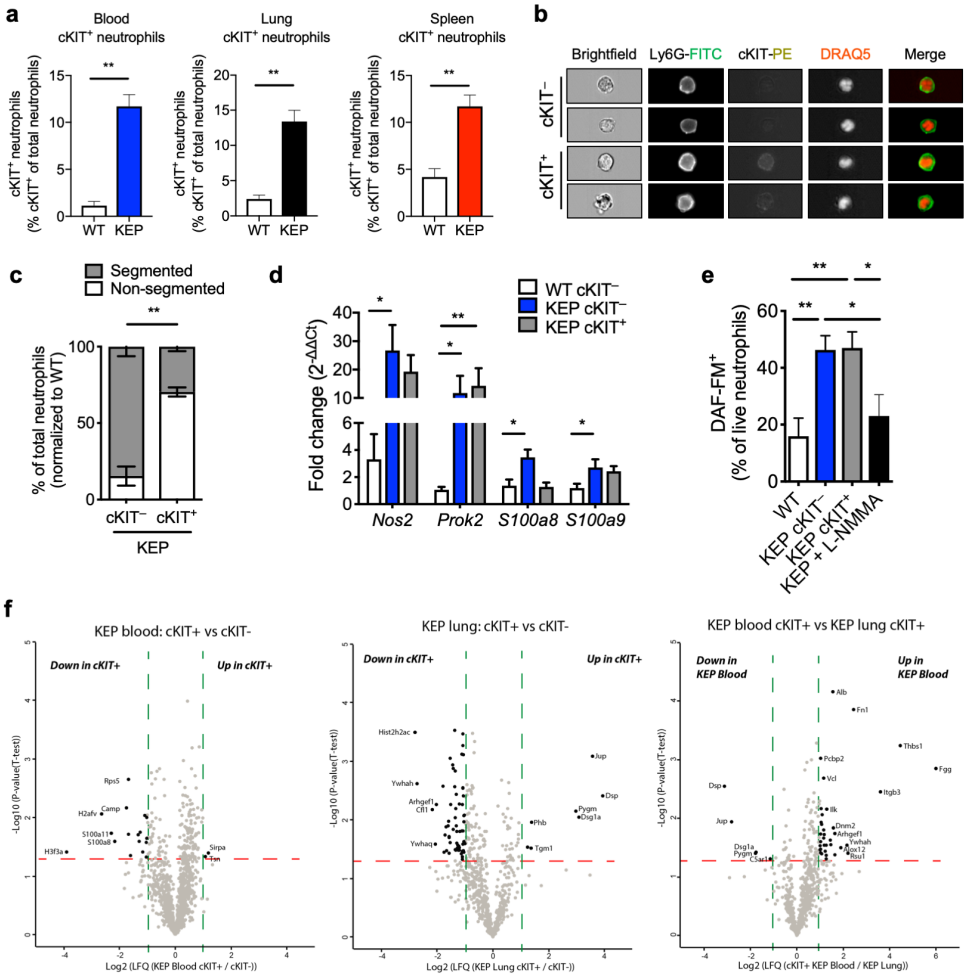

Mammary tumors induce expansion of immature cKIT+ neutrophils with tissue-specific protein expression

We previously observed that mammary tumor-activated neutrophils expressed cKIT on their cell surface, a protein that under homeostatic conditions is only expressed on neutrophil progenitor cells in the bone marrow[15,35,40]. Indeed, we detected cKIT expressing neutrophils in circulation, lungs and spleen of mice with orthotopically transplanted KEP tumors, while these are largely absent in WT controls (**Fig. 8.3a**). Because cKIT is expressed on neutrophil progenitor cells, we next assessed the nuclear morphology of these cells in circulation, as a readout for their maturation status[30]. Using ImageStream analysis, we observed that cKIT+ neutrophils from circulation were strongly enriched for a non-segmented nuclear morphology compared to cKIT– neutrophils (**Fig. 8.3b, c**), suggesting that these cells are less differentiated. However, ±25% of cKIT+ neutrophils still displayed segmented nuclei, indicating that cKIT does not exclusively mark immature neutrophils (**Fig. 8.3c**).

Having established that neutrophils can adapt tissue-specific gene and protein expression profiles, we sought to determine whether cKIT-expressing neutrophils differ from their cKIT-negative counterparts, and whether they display tissue-specific phenotypes. To this end, we first isolated cKIT+ and cKIT– neutrophils from the circulation of tumor-bearing mice and cKIT– neutrophils from WT mice and assessed expression of *Nos2, Prok2, S100a8* and *S100a9.* We observed consistent upregulation of *Nos2, Prok2* and *S100a9* in neutrophils from KEP tumor-bearing mice, but no marked differences between cKIT+ and cKIT– neutrophils (**Fig. 8.3d**). Only *S100a8* was upregulated in cKIT–, but not in cKIT+ neutrophils (**Fig. 8.3d**). Because neutrophils exert their pro-metastatic function in KEP mice mainly by NO-induced suppression of T cells[15], we next assessed NO levels in cKIT+ and cKIT– neutrophils from blood using the molecular probe 4-Amino-5-Methylamino-2',7'-Difluorofluorescein diacetate (DAF-FM). While NO levels were significantly increased in KEP neutrophils compared to WT neutrophils, and reduced by addition of iNOS inhibitor L-N^G-monomethyl-arginine (L-NMMA), we detected no difference in NO levels between cKIT+ and cKIT– neutrophils (**Fig. 8.3e**), consistent with *Nos2* being expressed to an equal extent (**Fig. 8.3d**). This suggests that expression of cKIT does not mark neutrophils that are altered in their immunosuppressive capabilities.

To obtain a more unbiased insight into the potential differences between these cells, we subjected lung and blood cKIT+ and cKIT– neutrophils to LC-MS/MS analysis. In blood, we observed that cKIT+ neutrophils have a lower expression level of certain effector proteins associated with fully differentiated neutrophils, such as S100a8 and S100a11 (**Fig. 8.3f, Supplemental Fig. 8.1c**). In lungs, proteins associated with cellular adhesion were most significantly upregulated in cKIT+ neutrophils, while cKIT– neutrophils were enriched for enzymatic activity (**Fig. 8.3f, Supplemental Fig. 8.1c**). When comparing cKIT+ neutrophils from blood with those from lungs, differentially expressed proteins mainly related to protein binding processes (**Fig. 8.3f, Supplemental Fig. 8.1c**). Overall, these data show that there are few but significant changes in protein expression between cKIT+ and cKIT– neutrophils, and that these cells also alter their proteome according to the anatomical location in which they reside.

Targeting cKIT impairs mammary tumor growth and pulmonary metastasis

Because targeting neutrophils in KEP mice reduces metastasis[15,35,60], and we observed differences in neutrophil phenotype depending on the expression of cKIT on their cell surface,

we wondered if we could assess the impact of cKIT+ neutrophils on tumor progression and metastasis by disrupting the Stem Cell Factor (SCF)-cKIT axis. To this end, we transplanted KEP tumor fragments orthotopically and treated mice with established tumors with ACK2, a monoclonal antibody directed against cKIT (**Fig. 8.4a**). During treatment, when tumors were 50 mm^2, the effect of ACK2 treatment on circulating cell populations was determined. ACK2 did not reduce the frequency of cKIT+ neutrophils, nor of total cKIT-expressing cell in circulation at this timepoint during the treatment (**Supplemental Fig. 8.2a**). To evaluate potential direct targeting of cancer cells expressing cKIT by ACK2, we also measured cKIT expression on $CD45^-$ cells in untreated KEP tumors. Overall, $CD45^-$ cells exhibited low cKIT expression, at levels significantly lower than observed on neutrophils in KEP tumors (**Supplemental Fig. 8.2b**). This suggests that ACK2 will have a limited effect on cancer cells themselves. Despite the lack of depletion of cKIT-expressing immune cells in circulation, primary tumors showed a modest delay in outgrowth in ACK2-treated mice (**Fig. 8.4b**). Moreover, metastasis to lungs was significantly reduced and incidence of lymph node metastasis showed a trend towards decrease in ACK2-treated mice (**Fig. 8.4c, d**). This suggests that, while ACK2 treatment did not impair the mobilization of cKIT+ cells in circulation, it may have hampered cKIT signaling function or mobilization in tissue, which was not assessed. Although we have not shown which cells specifically are targeted by this antibody, ACK2 treatment shows the potential to slow primary tumor development and impede metastasis formation to the lungs.

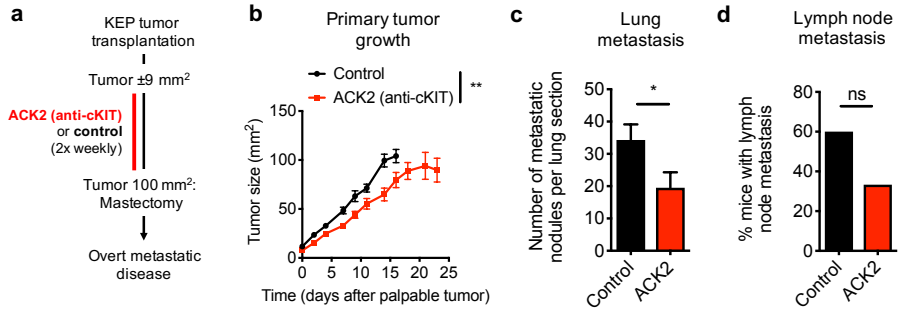

Figure 8.4. ACK2-mediated inhibition of the SCF-cKIT axis impairs primary tumor growth and metastasis. a. Experimental setup for neo-adjuvant inhibition of cKIT signaling in KEP tumor-bearing mice using ACK2 (100 µg/injection, twice weekly, intraperitoneal). Treatment was initiated when tumors were ±9 mm^2 and terminated upon mastectomy when tumors were 100 mm^2. **b.** Primary tumor growth kinetics during treatment with ACK2 or control (n=13–15/group). **c.** Number of cytokeratin-8+ metastatic nodules in lungs of mice treated with ACK2 or control (n=10/group). **d.** Incidence of metastasis to axillary lymph nodes in mice treated with ACK2 or control (n=10/group). All data are ± S.E.M.; * $P < 0.05$, ** $P < 0.01$, as determined by Area Under the Curve (AUC) calculation, followed by Student's t-test (**b**), Mann-Whitney test (**c**), or χ^2-test (**d**).

Discussion

Neutrophils play an imperative role in cancer development and metastasis, but due to their diverse phenotypes and high plasticity, using these cells in anti-cancer immunotherapeutic strategies remains challenging. In this work, we aimed to shed light on neutrophil diversity in breast cancer and how this may ultimately impact disease progression. We have shown that neutrophils can adapt phenotypes tailored to the anatomical location in which they reside and that tumor-derived signals can override this tissue-specific activation state. Moreover,

we present early evidence that cKIT may label a tumor-induced subpopulation of neutrophils with a unique phenotype in terms of differentiation and protein expression.

Upon examination of tissue-specific proteomic profiles of neutrophils, we observed marked differences between circulating and lung neutrophils in non-tumor-bearing animals (**Fig. 8.2e**). Interestingly, in tumor-bearing hosts the proteome of neutrophils from blood and lungs is largely comparable (**Fig. 8.2f**). This may indicate that in cancer-induced systemic neutrophilia, the rapid mobilization of neutrophils and their progenitor cells causes systemic accumulation of cells with a relatively homogenous proteome profile. Interestingly, in the B16F1 melanoma model, systemically expanded neutrophils from blood, bone marrow and spleen showed similar gene expression profiles, while those that entered tumors were distinct from their peripheral counterparts[27]. Moreover, a recent study used single cell RNA sequencing (scRNAseq) on human and mouse lung cancer tissue to demonstrate at least five different neutrophil phenotypes within one tumor type, thereby demonstrating an unprecedented heterogeneity of intratumoral and circulating neutrophils at the transcriptome level[61]. Moreover, this analysis demonstrated that there is indeed transcriptomic overlap between neutrophils in lung tumors and those that are circulating, but that there are also phenotypes that are unique for each[61]. It would therefore be of interest to profile the proteome of KEP tumor-infiltrating neutrophils and to compare their proteomes to their circulating and lung counterparts on the protein level to assess whether this relative homogenous phenotype we observe in systemic neutrophils is maintained within KEP tumors. In addition, it will be important to determine the (loss of) diversity of mammary tumor-induced systemic neutrophil phenotypes between different tumor types on a single cell level. A recent scRNAseq analysis on neutrophils from the MMTV-PyMT breast cancer model has further revealed diverse transcriptomic profiles within intratumoral and systemic neutrophil populations, which only partially overlap[62]**.** These reports that characterize neutrophils in-depth on the single cell level raise the question whether this diversity reflects neutrophil plasticity and adaptability, or whether tumors induce different developmental programs that generate subsets of cells within the neutrophil population, or both. Moreover, the molecular cues that are that are coming from these different organs and tumors that induce this diversity, remain largely unknown.

In this study, we have not addressed the functional relevance of the changes in protein expression we observed either in an organ-specific or a maturation state-specific manner. One aspect of diversity we observed in the proteins expressed by neutrophils pertained to metabolic pathways (**Supplemental Fig. 8.1a**). Metabolic reprogramming of neutrophils can alter their functional impact on cancer[63]. We observed altered metabolic pathways in neutrophils of tumor-bearing mice, such as decreased arachidonate lipoxygenase (ALOX) activity in blood (**Supplemental Fig. 8.1a**). ALOX proteins participate in metabolism of arachidonic acid by acting on Leukotriene A4 (LTA4). While in KEP-induced circulating neutrophils ALOX metabolism was decreased, other studies have shown this pathway to be induced by tumors. For example, activation of this metabolic pathway has recently been linked to the induction of an immunosuppressive phenotype in tumor-associated neutrophils in several transplantable and transgenic murine cancer models[59]. This is in contrast to the reduction of ALOX metabolism we observe in circulating neutrophils in the KEP model, and therefore may indicate that ALOX proteins and metabolism of arachidonic acid in neutrophils is tumor model-specific. Another ALOX protein that is expressed by neutrophils in the MMTV-PyMT breast cancer mouse model, ALOX5, was shown to promote metastasis to the lung

by enriching for metastasis-initiating cells[16]. ALOX5 is also up-regulated in KEP-induced neutrophils in lungs, but not in blood (**Fig. 8.2d**), and hence may also play a role in metastasis of KEP tumors. Lung neutrophils also show an increase in several other metabolic pathways, including but not limited to superoxide generation (**Supplemental Fig. 8.1a**). Interestingly, others have shown that 4T1 mammary tumor-induced cKIT$^+$ neutrophils have increased mitochondrial metabolism as a result of tumor-derived SCF, which enhances reactive oxygen species (ROS) production[36]. Similarly, this same study showed that ovarian cancer patients also exhibit immature CD10$^+$ neutrophils with increased mitochondrial respiration[36]. It would therefore be of interest to determine if that link also exists in KEP mice and if this is restricted to certain organs, such as the lungs. Together, the proteomic profiling performed in this study underscores that tumors alter neutrophil metabolism and that metabolic reprogramming in neutrophils may play a seminal role in their function in cancer.

Immunosuppression by neutrophils is a major aspect of their tumor-promoting capacities[1]. KEP tumor-induced expression of iNOS was mainly observed in blood and lung neutrophils, but not in spleen neutrophils (**Fig. 8.1b**). Tumor-induced immature neutrophils have been reported by others to be more immunosuppressive[32]. While cKIT$^+$ neutrophils exhibit a nuclear morphology that indicates an immature phenotype (**Fig. 8.3b, c**), both cKIT$^+$ and cKIT$^-$ neutrophils exhibited equally high levels of NO production (**Fig. 8.3d, e**). This is intriguing, since one analysis revealed that the immunosuppressive function of myeloid cells can already be observed in common myeloid progenitors (CMPs) and granulocyte-monocyte progenitors (GMPs) under homeostatic conditions[64]. This immunosuppressive function of CMPs and GMPs is further enhanced by the presence of a tumor and largely mediated by NO production in both subcutaneous lung tumor-bearing, but intriguingly also non-tumor bearing animals[64]. Because mammary tumor-derived signals alter myelopoiesis in the bone marrow, resulting in increased generation and release of myeloid progenitor cells[37], one could hypothesize that this would result in the release of not fully differentiated –and therefore immunosuppressive– neutrophils. However, we observed no difference in NO levels in neutrophils that express cKIT and those that do not (**Fig. 8.3d, e**), so it is likely that NO-mediated immunosuppression is induced early in neutrophil maturation and maintained, hence showing equally high NO-production in mature (cKIT$^-$) and immature (cKIT$^+$) neutrophils. Nevertheless, other immunosuppressive mechanisms, such those mediated by Arginase-1, were not considered in this study and therefore remain to be addressed in these cells.

Although immunosuppressive molecules are expressed in equal fashion between cKIT$^+$ and cKIT$^-$ neutrophils, our analysis indicates subtle differences in protein production, resulting in activation of an array of different signaling pathways (**Supplemental Fig. 8.1b**). One could therefore speculate that these subsets of neutrophils may behave in a distinct manner. It has been reported that transplanted E0771 breast tumors activate and expand hematopoietic progenitor cells within the pre-metastatic niche, and these cells were able to differentiate into immunosuppressive neutrophils[65]. Whether cKIT$^+$ neutrophils are able to differentiate into cKIT$^-$ neutrophils *in situ* remains to be established. Analyses into the nature of cKIT-expressing neutrophils using scRNAseq and mass cytometry have elegantly shown that a distinct neutrophil progenitor marked among others by cKIT has unique functions, including chemotaxis, phagocytosis, ROS production, and indeed support of tumor growth[38,41]. However, it must be noted that cKIT does not fully enrich for immature neutrophils (**Fig. 8.3c**) and using a combination of other markers, such as CD101[38], may improve this.

Nonetheless, these studies and ours provide early evidence that cKIT marks a functionally distinct neutrophil subset, which may be interesting to target in tumor-bearing hosts.

Targeting cKIT-expressing neutrophils has shown promise in various cell line-based mouse tumor models, including the 4T1 mammary cancer and CT26 colon cancer models[42,66]. These reports found that tumor-derived SCF is required for recruitment of among others tumor-promoting neutrophils, and that genetic or antibody-mediated disruption of SCF-cKIT signaling reversed this recruitment[42,66]. Our work presented here also hints that targeting the SCF-cKIT axis may reduce tumor growth and metastasis, although it remains to be established whether this effect is due to targeting cKIT$^+$ neutrophils specifically, since we did not observe depletion of cells that express this receptor from circulation during ACK2 treatment. It would therefore be of interest to assess deactivation of the cKIT pathway in neutrophils, as its signaling may be impaired by ACK2 treatment. Although ACK2 was originally described not to be toxic to cKIT$^+$ cells at the doses used in this study, but rather inhibits cKIT function[67], this antibody has been shown to deplete cKIT-expressing cells from the bone marrow at higher doses[68,69]. Therefore, it is also possible that developing immune cells in the bone marrow of KEP tumor-bearing mice are targeted by ACK2. Moreover, there are other cell types that express cKIT in peripheral tissues, such as mast cells, which have also been shown to play an important role in breast cancer[70]. In addition, while cancer cells from primary KEP tumors are largely cKIT$^-$ (**Supplemental Fig. 8.2b**), metastasizing cancer cells can potentially acquire cKIT expression[71]. Importantly, it is of note that we have previously shown that antibody-mediated targeting of the entire neutrophil population in KEP mice did not affect primary tumor growth[15], while ACK2 treatment did affect tumor growth (**Fig. 8.4b**). Therefore, the anti-tumorigenic and anti-metastatic effect of ACK2 observed in this work requires further elucidation. However, rather than targeting the signaling of cKIT itself, this receptor is perhaps better used as a marker for tumor-induced neutrophils in the periphery, and effector molecules that these cells produce or their potential unique vulnerabilities may be better suitable for targeting.

To target tumor-induced neutrophils, several studies have used blockade of chemokine receptor CXCR2, since it is essential for their egress from the bone marrow[72]. Targeting CXCR2 has been shown to block metastasis-promoting neutrophils and improve anti-PD-1 therapy in mouse models for pancreatic cancer and sarcoma[73,74]. Although it is unknown whether cKIT-expressing neutrophils are induced by these tumors, it is important to note that CXCR2 is only expressed on terminally differentiated neutrophils and its expression anti-correlates with expression of cKIT during differentiation in the bone marrow[36,38]. Therefore, CXCR2 blockade may not target cKIT$^+$ neutrophils. While differences between cKIT$^+$ and cKIT$^-$ neutrophils in this work are minor and require further functional examination, we do observe a slight but significant upregulation of SIRPα protein levels in circulating cKIT$^+$ neutrophils (**Fig. 8.3f**). Interaction of this protein with its ligand CD47 negatively regulates phagocytosis of CD47-expressing cells. SIRPα blocking antibodies are actively being tested as an immunotherapy to engage phagocytosis of cancer cells by myeloid cells. Interestingly, blocking CD47-SIRPα signaling has been shown to increase the anti-tumor effect of neutrophils[75,76]. Although the upregulation of SIRPα is minor in KEP-induced cKIT$^+$ neutrophils, it may be an interesting therapeutic target to pursue in future studies.

This work, together with other studies, shows that the diversity of neutrophil phenotypes needs to be thoroughly examined in order to fruitfully employ these cells for anti-cancer therapies. Comprehensive analysis of neutrophils using scRNAseq has revealed and will

further reveal the vast degrees of complexity in gene expression profiles in different disease entities, including cancer[41,61,62]. Further assessment of the neutrophil proteome during differentiation and disease-mediated reprogramming as shown in this work and by others[77-79] may reveal novel therapeutic targets and molecules that can be used for identification and characterization of neutrophil progenitor cells. Importantly, examining neutrophils using these high-resolution methodologies will not only shed light on the many faces of this cell type, but can also be used to show if and to what extend these phenotypes are conserved between different patients, but also between mouse and human, as was done for lung cancer[61]. This inter-species conservation is encouraging for studies using clinically relevant murine models and opens the way to functional validation of clinically-relevant neutrophil phenotypes in mice. This daunting task of understanding cells with such high levels of plasticity will ultimately help to improve anti-cancer immunotherapeutics.

Methods

Mouse studies

All animal studies were approved by the Animal Ethics Committee of the Netherlands Cancer Institute and performed in accordance with institutional, national and European guidelines for Animal Care and Use. All experiments were performed using *K14-cre;Cdh1$^{F/F}$;Trp53$^{F/F}$* (KEP) mice[44], the KEP-based spontaneous metastasis model[80] or wild-type (WT) age-matched FVB/N control mice. In this latter model, KEP tumor fragments of approximately 1 mm^2 were orthotopically transplanted into 10 – 12-week-old female recipient WT FVB/N mice. These tumor pieces were allowed to grow out, then surgically removed at 100 mm^2, after which mice are monitored until development of metastatic disease. Tumor sizes were measured twice weekly using calipers. For cKIT targeting studies, KEP tumors were transplanted as noted above and when tumors reached a size of 9 mm^2, 100 µg anti-cKIT antibody (ACK2, Biolegend) was injected three times per week intraperitoneally (i.p.) until mastectomy. Animals were randomized at the beginning the treatment. Sample sizes were predetermined based on previous experience with this model[15,60]. Metastasis was scored in lungs by counting cytokeratin-8 (K8)-positive nodules in tissue sections of lungs and axillary lymph nodes (see below). Micrometastatic nodules containing <10 K8+ cells were not considered as metastasis, nodules with >10 cells and macrometastases were counted as metastasis. Mice were excluded from metastasis analysis when they succumbed to non-metastasis-related causes, such as surgery-related death or death due to recurrence of primary tumors after surgery. Mice were kept in individually ventilated and open cages and food and water were provided *ad libitum*.

Flow cytometry

Tissues (lungs and spleens) were collected in PBS and blood in heparin-containing tubes. Lungs were mechanically chopped using a McIlwain tissue chopper (Mickle Laboratory Engineering), followed by digestion for 30 minutes (min) at 37°C in Liberase TM (Roche). Enzyme reactions were stopped by addition of cold DMEM/8% Fetal Calf Serum (FCS) and suspensions were dispersed through a 70 µm cell strainer. Spleens were mashed through a 70 µm cell strainer to generate single cell suspensions. Lungs, spleen and blood were treated with NH_4Cl erythrocyte lysis buffer twice for 5 min at room temperature (RT). Before staining, cell suspensions were subjected to Fc receptor blocking (rat anti-mouse CD16/32, BD Biosciences) for 15 min at 4°C. Cells were stained with conjugated antibodies for 30 min at 4°C in the dark in PBS/0.5% BSA. The following antibodies were used in the experiments: CD45-eFluor 605NC (1:50; clone 30-F11, eBioscience), CD11b-eFluor 650NC (1:400; clone M1/70, eBioscience), Ly6G-AlexaFluor 700 (1:400; clone 1A8, Biolegend), Ly6C-eFluor 450 (1:400; clone HK1.4, eBioscience), cKIT-PE-Cy7 (1:400; clone 2B8, eBioscience). 7AAD (1:20, eBioscience) was added to exclude dead cells.

To measure nitric oxide (NO) production, white blood cells from blood of KEP or WT mice were stained for cell surface proteins (anti-Ly6G-APC (clone 1A8, 1:200, eBioscience/ThermoFisher), anti-CD11b-APC-Cy7 (clone M1/70, 1:400, eBioscience/ThermoFisher), anti-cKIT-PE (clone 2B8, 1:200, eBioscience/ThermoFisher)), washed, followed by incubation of with 1 µM DAF-FM diacetate molecular probe (Invitrogen/ThermoFisher) per 1 x 10^6 total blood cells for 30 min at 37°C and 15 min de-esterification. Where indicated, cells were pre-treated for 1 h with 0.5 mM iNOS inhibitor L-N^G-monomethyl-arginine (L-NMMA, Sigma). All experiments were performed using a BD LSR II flow cytometer using Diva software. Data

analyses were performed using FlowJo Software (version 9.9).

RNA isolation and RT-qPCR

RNA from sorted total neutrophils or cKIT$^+$ and cKIT$^-$ neutrophils from lungs, spleen and blood from KEP and WT mice was isolated using TRIzol and phenol-chloroform extraction, followed by treatment with DNase I (Invitrogen). RNA concentration and quality were measured with a 2100 Bioanalyzer from Agilent. RNA was converted to complementary DNA (cDNA) with an AMV reverse transcriptase using Oligo(dT) primers (Invitrogen). cDNA (20 ng per well) was analyzed by SYBR green real-time PCR with 500 nM primers using a LightCycler 480 thermocycler (Roche). The following primer sequences were used:
Nos2 forward (FW): 5'-GTTCTCAGCCCAACAATACAAGA-3', *Nos2* reverse (RV): 5'-GTGGA CGGGTCGATGTCAC-3', *Prok2*FW: 5'-CTTCGCCCTTCTTCTTTCCT-3', *Prok2*RV: 5'-GCATGT GCTGTGCTGTCAGT-3', *S100a8* FW: 5'-TGAGCAACCTCATTGATGTCTACC-3', *S100a8* RV: 5'-ATGCCACACCCACTTTTATCACC-3', *S100a9* FW: 5'-GAAGAAAGAGAAGAGAAATGAAG CC-3', *S100a9* RV: 5'-CTTTGCCATCAGCATCATACACTCC-3'. As a reference gene, β-actin (*Actb*) was used, with FW: 5'- CCTCATGAAGATCCTGACCGA-3' and RV: 5'-TTTGATGTCACGCACGATTTC-3'. Fold change in expression was calculated using $2^{-(\Delta Ct.gene\ x - average[\Delta Ct.control])}$.

ImageStream analysis

To analyze the nuclear morphology of circulating neutrophils, blood cells were isolated from transgenic KEP mice bearing 100 mm^2 tumors and WT age-matched controls and processed as described above and subsequently labeled with anti-Ly6G-FITC (clone 1A8, 1:200, eBioscience/ThermoFisher) and anti-cKIT-PE (clone 2B8, 1:200, eBioscience/ ThermoFisher)). Cell-permeable DRAQ5 (ThermoFisher, 1:1000) was used to stain nuclei and DAPI was used to exclude dead cells. Next, cells were analyzed on an ImageStream^X Mark II imaging flow cytometer (Merck) and nuclear morphology was analyzed using IDEAS V6.2 Software (Merck) by training the software to distinguish segmented and non-segmented nuclei. Samples from WT mice, which do not contain cKIT$^+$ neutrophils in blood, were used to gate for cKIT expressing neutrophils and normalize nuclear morphology data.

Mass spectrometry

Total neutrophils were isolated from blood and lungs of from transgenic KEP mice bearing 100 mm^2 tumors or WT age-matched control mice by magnetic activated cell sorting (MACS) using anti-Ly6G-APC primary antibodies (eBioscience/ThermoFisher) and anti-APC beads (Miltenyi Biotec). cKIT$^+$ and cKIT$^-$ neutrophils were isolated from blood and lungs of transgenic KEP tumor-bearing or WT control mice by fluorescence activated cell sorting (FACS) using the following antibodies: anti-CD11b-APC, anti-Ly6G-FITC anti-cKIT-PE and 7AAD to exclude dead cells. Tissues were prepared as described above. Cells were washed once in PBS and snap-frozen.

Neutrophil cell pellets were lysed and proteins were reduced and alkylated by heating at 95°C for 5 min in lysis buffer (1% SDC, 10 mM TCEP, 40 mM chloroacetamide, 100mM Tris pH 8.5). Lysates were tip sonicated, cell debris was pelleted and supernatants were diluted 10 times with 50 mM ammonium bicarbonate containing Lys-C (Wako; 1:75) and trypsin (Sigma; 1:50). Proteins were digested overnight at 37°C. After acidification (1% TFA), digests were desalted on a Sep-Pak C18 cartridge (Waters, Massachusetts, USA). Peptides were

vacuum dried and stored at -80°C until LC-MS/MS analysis.

Peptides were reconstituted in 2% formic acid and analyzed by nanoLC-MS/MS on an Orbitrap Fusion Tribrid mass spectrometer equipped with an Easy-nLC1000 system (Thermo Scientific). Samples were directly loaded onto the analytical column (ReproSil-Pur 120 C18-AQ, 2.4 µm, 75 µm × 500 mm, packed in-house). Solvent A was 0.1% formic acid/water and solvent B was 0.1% formic acid/80% acetonitrile. Peptides were eluted from the analytical column at a constant flow of 250 nl/min. For single-run proteome analysis, a 4h gradient was employed containing a linear increase from 5% to 35% solvent B, followed by a 15-min wash. The mass spectrometer was run in top speed mode with 3 s cycles. Survey scans of peptide precursors from m/z 375-1500 were performed at 120K resolution with a 4 x 105 ion count target. Tandem MS was performed by quadrupole isolation at 1.6 Th, followed by HCD fragmentation with normalized collision energy 33 and ion trap MS2 fragment detection. The MS2 ion count target was set to 104 and the max injection time was set to 100 ms. Only precursors with charge state 2-6 were sampled for MS2. Monoisotopic precursor selection was turned on; the dynamic exclusion duration was set to 60s with a 10 ppm tolerance around the selected precursor and its isotopes.

RAW files were analyzed with label-free quantification (LFQ) using MaxQuant (version 1.5.0.30)[81] using standard settings. Spectra were searched against the mouse Swissprot database (release 2016_02); trypsin was chosen as cleavage specificity allowing two missed cleavages; carbamidomethylation (C) was set as fixed modification, whereas oxidation (M) and protein N-terminal acetylation were set as variable modifications. The MaxQuant output file containing LFQ abundances was loaded into Perseus (version 1.5.0.31)[82]. Abundances were Log_2-transformed and the proteins were filtered for at least three out of four valid values in one condition. Missing values were replaced by imputation based on the standard settings of Perseus, i.e. a normal distribution using a width of 0.3 and a downshift of 1.8. Differential proteins were determined using a two-sided Student's t-test (threshold: $p < 0.05$ and $[x/y] > 1 \mid [x/y] < -1$).

Immunohistochemistry

Formalin-fixed tissues were processed by routine procedures by the NKI Animal Pathology Facility. 4 µm sections were stained using anti-cytokeratin 8 (clone Troma 1, DHSB University of Iowa). Citrate buffer was used for antigen retrieval. Lungs and axillary lymph nodes were analyzed for presence of metastatic nodules by assessing cytokeratin-8-positive cancer cells by three independent researchers.

Statistics

Statistical analyses were performed using GraphPad Prism (version 8) using statistical tests indicated in the figure legends. Generally, comparison of two groups was performed using Mann-Whitney test, Student's t-test or χ^2 test, more than two group were compared using one-way ANOVA, tumor growth curves were analyzed comparing the area under the curve (AUC) followed by t-test. All statistical tests were two-tailed. Differences with $P < 0.05$ were considered statistically significant. Heatmap generation and principal component analysis were performed using Qlucore Omics Explorer (version 3.5). Gene ontology analysis of differentially expressed proteins was performed using GO enrichment analysis (http://geneontology.org)[83,84] for up- and down-regulated biological processes (*Mus musculus*) separately.

Acknowledgements
Research in the De Visser laboratory is funded by a European Research Council Consolidator award (ERC InflaMet 615300), the Netherlands Organization for Scientific Research (NWO-VICI 91819616), Oncode Institute and the Dutch Cancer Society (KWF10083; KWF10623). The proteomics work in this study was supported by the X-omics Initiative, co-funded by the Netherlands Organization for Scientific Research (NWO 184034019). We thank the flow cytometry facility, genomics facility, proteomics facility, animal laboratory facility and animal pathology facility of the Netherlands Cancer Institute for technical assistance.

Acknowledgements
M.D.W, S.B.C. and K.E.d.V. conceived the ideas and designed the experiments. M.D.W., S.B.C. performed animal experiments, flow cytometry, cell sorting, RT-qPCR, ImageStream and ACK2 intervention experiments and analyzed the data. M.D.W., O.B.B. and M.A. performed mass spectrometry analysis of total neutrophil populations, M.D.W., H.G., O.B.B. and M.A. performed sorting and mass spectrometry analysis of cKIT^{-} and cKIT^{+} neutrophils. C.-S.H. and K.V. performed mouse experiments and provided technical support. K.E.d.V. supervised the study and acquired funding. M.D.W. and K.E.d.V. wrote the paper and prepared the figures.

Supplemental Data

Supplemental Figure 8.1. Gene ontology analysis of differentially expressed proteins in neutrophils from blood and lung. a, b. Gene ontology (GO) term analysis showing top enriched pathways of differentially expressed proteins comparing blood neutrophils (**a**) and lung neutrophils (**b**) from KEP and WT mice. **c.** GO term analysis of differentially expressed showing top enriched pathways between blood and lung neutrophils in WT mice. **d – f.** GO term analysis of differentially expressed showing top enriched pathways between cKIT$^+$ and cKIT$^-$ neutrophils from blood (**d**) and lung (**e**) and comparing cKIT$^+$ neutrophils from blood and lung (**f**), isolated from KEP mice.

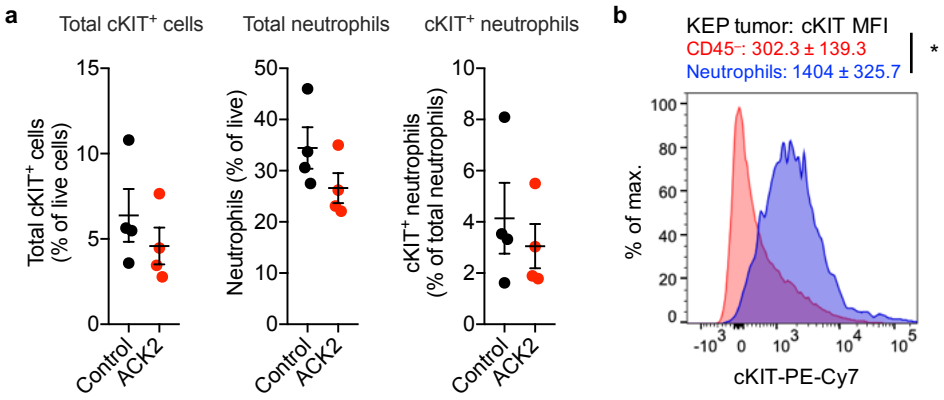

Supplemental Figure 8.2. ACK2-mediated targeting of cKIT signaling does not lead to depletion of cKIT⁺ cells from circulation. a. Frequency of all cKIT-expressing cells (% of total live cells), total neutrophils (% $CD11b^{+}Ly6G^{+}Ly6C^{low}$ of total live cells) and cKIT-expressing neutrophils (% of $cKIT^{+}$ of total live $CD11b^{+}Ly6G^{+}Ly6C^{low}$ cells) in blood of mice bearing 50 mm^2 tumors measured 24 hours after treatment (n=4/group). **b.** Histogram showing the difference in cKIT expression on $CD45^{-}$ cells and neutrophils in an untreated KEP tumor, with median fluorescence intensity (MFI) indicated (n=3/group). All data are ± S.E.M.; * $P < 0.05$, ** $P < 0.01$, as determined by two-sided Mann-Whitney test (**a**) or Student's t-test (**b**).

References

1. Coffelt, S.B., Wellenstein, M.D. & de Visser, K.E. Neutrophils in cancer: neutral no more. *Nat. Rev. Cancer* **16**, 431–446 (2016).
2. Gentles, A.J., *et al.* The prognostic landscape of genes and infiltrating immune cells across human cancers. *Nat. Med.* **21**, 938-945 (2015).
3. Granot, Z., *et al.* Tumor entrained neutrophils inhibit seeding in the premetastatic lung. *Cancer Cell* **20**, 300-314 (2011).
4. Finisguerra, V., *et al.* MET is required for the recruitment of anti-tumoural neutrophils. *Nature* **522**, 349-353 (2015).
5. Blaisdell, A., *et al.* Neutrophils Oppose Uterine Epithelial Carcinogenesis via Debridement of Hypoxic Tumor Cells. *Cancer Cell* **28**, 785-799 (2015).
6. Ponzetta, A., *et al.* Neutrophils Driving Unconventional T Cells Mediate Resistance against Murine Sarcomas and Selected Human Tumors. *Cell* (2019).
7. Yang, L., *et al.* Expansion of myeloid immune suppressor Gr+CD11b+ cells in tumor-bearing host directly promotes tumor angiogenesis. *Cancer Cell* **6**, 409-421 (2004).
8. Nozawa, H., Chiu, C. & Hanahan, D. Infiltrating neutrophils mediate the initial angiogenic switch in a mouse model of multistage carcinogenesis. *Proc. Natl. Acad. Sci. U. S. A.* **103**, 12493-12498 (2006).
9. Shojaei, F., *et al.* Bv8 regulates myeloid-cell-dependent tumour angiogenesis. *Nature* **450**, 825-831 (2007).
10. Fridlender, Z.G., *et al.* Polarization of tumor-associated neutrophil phenotype by TGF-beta: "N1" versus "N2" TAN. *Cancer Cell* **16**, 183-194 (2009).
11. Kowanetz, M., *et al.* Granulocyte-colony stimulating factor promotes lung metastasis through mobilization of Ly6G+Ly6C+ granulocytes. *Proc. Natl. Acad. Sci. U. S. A.***107**, 21248-21255 (2010).
12. Houghton, A.M., *et al.* Neutrophil elastase-mediated degradation of IRS-1 accelerates lung tumor growth. *Nat. Med.* **16**, 219-223 (2010).
13. Di Mitri, D., *et al.* Tumour-infiltrating Gr-1+ myeloid cells antagonize senescence in cancer. *Nature* **515**, 134-137 (2014).
14. Bald, T., *et al.* Ultraviolet-radiation-induced inflammation promotes angiotropism and metastasis in melanoma. *Nature* **507**, 109-113 (2014).
15. Coffelt, S.B., *et al.* IL-17-producing gammadelta T cells and neutrophils conspire to promote breast cancer metastasis. *Nature* **522**, 345–348 (2015).
16. Wculek, S.K. & Malanchi, I. Neutrophils support lung colonization of metastasis-initiating breast cancer cells. *Nature* **528**, 413–417 (2015).
17. Park, J., *et al.* Cancer cells induce metastasis-supporting neutrophil extracellular DNA traps. *Sci. Transl. Med.* **8**, 361ra138 (2016).
18. Steele, C.W., *et al.* CXCR2 Inhibition Profoundly Suppresses Metastases and Augments Immunotherapy in Pancreatic Ductal Adenocarcinoma. *Cancer Cell* **29**, 832-845 (2016).
19. Templeton, A.J., *et al.* Prognostic role of neutrophil-to-lymphocyte ratio in solid tumors: a systematic review and meta-analysis. *J. Natl. Cancer Inst.* **106**, dju124 (2014).
20. Jensen, H.K., *et al.* Presence of intratumoral neutrophils is an independent prognostic factor in localized renal cell carcinoma. *J. Clin. Oncol.* **27**, 4709-4717 (2009).
21. Carus, A., *et al.* Tumor-associated neutrophils and macrophages in non-small cell lung cancer: no immediate impact on patient outcome. *Lung Cancer* **81**, 130-137 (2013).
22. Droeser, R.A., *et al.* High myeloperoxidase positive cell infiltration in colorectal cancer is an independent favorable prognostic factor. *PLoS ONE* **8**, e64814 (2013).
23. Rao, H.L., *et al.* Increased intratumoral neutrophil in colorectal carcinomas correlates closely with malignant phenotype and predicts patients' adverse prognosis. *PLoS ONE* **7**, e30806 (2012).
24. Casanova-Acebes, M., *et al.* Neutrophils instruct homeostatic and pathological states in naive tissues. *J. Exp. Med.* (2018).
25. Adrover, J.M., *et al.* A Neutrophil Timer Coordinates Immune Defense and Vascular Protection. *Immunity* **50**, 390-402 e310 (2019).
26. Becher, B., *et al.* High-dimensional analysis of the murine myeloid cell system. *Nat. Immunol.* **15**, 1181-1189 (2014).

27. Glodde, N., *et al.* Reactive Neutrophil Responses Dependent on the Receptor Tyrosine Kinase c-MET Limit Cancer Immunotherapy. *Immunity* **47**, 789-802 e789 (2017).
28. Elpek, K.G., *et al.* The tumor microenvironment shapes lineage, transcriptional, and functional diversity of infiltrating myeloid cells. *Cancer Immunol. Res.* **2**, 655-667 (2014).
29. Mackey, J.B.G., Coffelt, S.B. & Carlin, L.M. Neutrophil Maturity in Cancer. *Front. Immunol.* **10**, 1912 (2019).
30. Pillay, J., Tak, T., Kamp, V.M. & Koenderman, L. Immune suppression by neutrophils and granulocytic myeloid-derived suppressor cells: similarities and differences. *Cell. Mol. Life Sci.* **70**, 3813-3827 (2013).
31. Manz, M.G. & Boettcher, S. Emergency granulopoiesis. *Nat. Rev. Immunol.* **14**, 302-314 (2014).
32. Sagiv, J.Y., *et al.* Phenotypic diversity and plasticity in circulating neutrophil subpopulations in cancer. *Cell Rep.* **10**, 562-573 (2015).
33. Youn, J.I., Collazo, M., Shalova, I.N., Biswas, S.K. & Gabrilovich, D.I. Characterization of the nature of granulocytic myeloid-derived suppressor cells in tumor-bearing mice. *J. Leukoc. Biol.* **91**, 167-181 (2012).
34. Wu, W.C., *et al.* Circulating hematopoietic stem and progenitor cells are myeloid-biased in cancer patients. *Proc. Natl. Acad. Sci. U. S. A.* **111**, 4221-4226 (2014).
35. Wellenstein, M.D., *et al.* Loss of p53 triggers WNT-dependent systemic inflammation to drive breast cancer metastasis. *Nature* **572**, 538-542 (2019).
36. Rice, C.M., *et al.* Tumour-elicited neutrophils engage mitochondrial metabolism to circumvent nutrient limitations and maintain immune suppression. *Nat. Commun.* **9**, 5099 (2018).
37. Casbon, A.J., *et al.* Invasive breast cancer reprograms early myeloid differentiation in the bone marrow to generate immunosuppressive neutrophils. *Proc. Natl. Acad. Sci. U. S. A.* **112**, E566-575 (2015).
38. Evrard, M., *et al.* Developmental Analysis of Bone Marrow Neutrophils Reveals Populations Specialized in Expansion, Trafficking, and Effector Functions. *Immunity* **48**, 364-379 e368 (2018).
39. Pember, S.O., Barnes, K.C., Brandt, S.J. & Kinkade, J.M., Jr. Density heterogeneity of neutrophilic polymorphonuclear leukocytes: gradient fractionation and relationship to chemotactic stimulation. *Blood* **61**, 1105-1115 (1983).
40. Ueda, Y., Kondo, M. & Kelsoe, G. Inflammation and the reciprocal production of granulocytes and lymphocytes in bone marrow. *J. Exp. Med.* **201**, 1771-1780 (2005).
41. Zhu, Y.P., *et al.* Identification of an Early Unipotent Neutrophil Progenitor with Pro-tumoral Activity in Mouse and Human Bone Marrow. *Cell Rep.* **24**, 2329-2341 e2328 (2018).
42. Kuonen, F., *et al.* Inhibition of the Kit ligand/c-Kit axis attenuates metastasis in a mouse model mimicking local breast cancer relapse after radiotherapy. *Clin. Cancer Res.* **18**, 4365-4374 (2012).
43. Ethier, J.L., Desautels, D., Templeton, A., Shah, P.S. & Amir, E. Prognostic role of neutrophil-to-lymphocyte ratio in breast cancer: a systematic review and meta-analysis. *Breast Cancer Res.* **19**, 2 (2017).
44. Derksen, P.W., *et al.* Somatic inactivation of E-cadherin and p53 in mice leads to metastatic lobular mammary carcinoma through induction of anoikis resistance and angiogenesis. *Cancer Cell* **10**, 437-449 (2006).
45. Hiratsuka, S., Watanabe, A., Aburatani, H. & Maru, Y. Tumour-mediated upregulation of chemoattractants and recruitment of myeloid cells predetermines lung metastasis. *Nat. Cell Biol.* **8**, 1369-1375 (2006).
46. Turner, S.R., Campbell, J.A. & Lynn, W.S. Polymorphonulcear leukocyte chemotaxis toward oxidized lipid components of cell membranes. *J. Exp. Med.* **141**, 1437-1441 (1975).
47. Rossaint, J., Nadler, J.L., Ley, K. & Zarbock, A. Eliminating or blocking 12/15-lipoxygenase reduces neutrophil recruitment in mouse models of acute lung injury. *Crit. Care* **16**, R166 (2012).
48. Mishra, B.B., *et al.* Nitric oxide prevents a pathogen-permissive granulocytic inflammation during tuberculosis. *Nat. Microbiol.* **2**, 17072 (2017).
49. Zarbock, A., Polanowska-Grabowska, R.K. & Ley, K. Platelet-neutrophil-interactions: linking hemostasis and inflammation. *Blood Rev.* **21**, 99-111 (2007).
50. Berman, R., *et al.* MUC18 Regulates Lung Rhinovirus Infection and Inflammation. *PLoS One* **11**, e0163927 (2016).

51. Wu, Q., *et al.* A novel function of MUC18: amplification of lung inflammation during bacterial infection. *Am. J. Pathol.* **182**, 819-827 (2013).
52. Robichaud, N., *et al.* Translational control in the tumor microenvironment promotes lung metastasis: Phosphorylation of eIF4E in neutrophils. *Proc. Natl. Acad. Sci. U. S. A.* (2018).
53. Hu, N., *et al.* Differential expression of granulopoiesis related genes in neutrophil subsets distinguished by membrane expression of CD177. *PLoS ONE* **9**, e99671 (2014).
54. Zhou, G., *et al.* CD177(+) neutrophils as functionally activated neutrophils negatively regulate IBD. *Gut* **67**, 1052-1063 (2018).
55. Xie, Q., *et al.* Characterization of a novel mouse model with genetic deletion of CD177. *Protein Cell* **6**, 117-126 (2015).
56. Riese, R.J., *et al.* Cathepsin S activity regulates antigen presentation and immunity. *J. Clin. Invest.* **101**, 2351-2363 (1998).
57. Singhal, S., *et al.* Origin and Role of a Subset of Tumor-Associated Neutrophils with Antigen-Presenting Cell Features in Early-Stage Human Lung Cancer. *Cancer Cell* (2016).
58. Mihelic, M., Teuscher, C., Turk, V. & Turk, D. Mouse stefins A1 and A2 (Stfa1 and Stfa2) differentiate between papain-like endo- and exopeptidases. *FEBS Lett.* **580**, 4195-4199 (2006).
59. Veglia, F., *et al.* Fatty acid transport protein 2 reprograms neutrophils in cancer. *Nature* **569**, 73-78 (2019).
60. Kersten, K., *et al.* Mammary tumor-derived CCL2 enhances pro-metastatic systemic inflammation through upregulation of IL1beta in tumor-associated macrophages. *Oncoimmunology* **6**, e1334744 (2017).
61. Zilionis, R., *et al.* Single-Cell Transcriptomics of Human and Mouse Lung Cancers Reveals Conserved Myeloid Populations across Individuals and Species. *Immunity* **21**, 1117-1134 (2019).
62. Alshetaiwi, H., *et al.* Defining the emergence of myeloid-derived suppressor cells in breast cancer using single-cell transcriptomics. *Sci. Immunol.* **5** eaay6017 (2020).
63. Kumar, S. & Dikshit, M. Metabolic Insight of Neutrophils in Health and Disease. *Front. Immunol.* **10**, 2099 (2019).
64. Pu, S., *et al.* Identification of early myeloid progenitors as immunosuppressive cells. *Sci. Rep.* **6**, 23115 (2016).
65. Giles, A.J., *et al.* Activation of Hematopoietic Stem/Progenitor Cells Promotes Immunosuppression Within the Pre-metastatic Niche. *Cancer Res.* **76**, 1335-1347 (2016).
66. Pan, P.Y., *et al.* Reversion of immune tolerance in advanced malignancy: modulation of myeloid-derived suppressor cell development by blockade of stem-cell factor function. *Blood* **111**, 219-228 (2008).
67. Nishikawa, S., *et al.* In utero manipulation of coat color formation by a monoclonal anti-c-kit antibody: two distinct waves of c-kit-dependency during melanocyte development. *EMBO J.* **10**, 2111-2118 (1991).
68. Ogawa, M., *et al.* Expression and function of c-kit in hemopoietic progenitor cells. *J. Exp. Med.* **174**, 63-71 (1991).
69. Czechowicz, A., Kraft, D., Weissman, I.L. & Bhattacharya, D. Efficient transplantation via antibody-based clearance of hematopoietic stem cell niches. *Science* **318**, 1296-1299 (2007).
70. Aponte-Lopez, A., Fuentes-Panana, E.M., Cortes-Munoz, D. & Munoz-Cruz, S. Mast Cell, the Neglected Member of the Tumor Microenvironment: Role in Breast Cancer. *J. Immunol. Res.* **2018**, 2584243 (2018).
71. Pittoni, P., Piconese, S., Tripodo, C. & Colombo, M.P. Tumor-intrinsic and -extrinsic roles of c-Kit: mast cells as the primary off-target of tyrosine kinase inhibitors. *Oncogene* **30**, 757-769 (2011).
72. Eash, K.J., Greenbaum, A.M., Gopalan, P.K. & Link, D.C. CXCR2 and CXCR4 antagonistically regulate neutrophil trafficking from murine bone marrow. *J. Clin. Invest.* **120**, 2423-2431 (2010).
73. Steele, C.W., *et al.* CXCR2 inhibition suppresses acute and chronic pancreatic inflammation. *J. Pathol.* **237**, 85-97 (2015).
74. Highfill, S.L., *et al.* Disruption of CXCR2-mediated MDSC tumor trafficking enhances anti-PD1 efficacy. *Science Transl. Med.* **6**, 237ra267 (2014).
75. Ring, N.G., *et al.* Anti-SIRPalpha antibody immunotherapy enhances neutrophil and macrophage antitumor activity. *Proc. Natl. Acad. Sci. U. S. A.* **114**, E10578-E10585 (2017).
76. Matlung, H.L., *et al.* Neutrophils Kill Antibody-Opsonized Cancer Cells by Trogoptosis. *Cell*

Rep. **23**, 3946-3959 e3946 (2018).
77. Tak, T.*, et al.* Human CD62Ldim neutrophils identified as a separate subset by proteome profiling and in vivo pulse-chase labeling. *Blood* **129**, 3476-3485 (2017).
78. Hoogendijk, A.J.*, et al.* Dynamic Transcriptome-Proteome Correlation Networks Reveal Human Myeloid Differentiation and Neutrophil-Specific Programming. *Cell Rep.* **29**, 2505-2519 e2504 (2019).
79. Grabowski, P.*, et al.* Proteome Analysis of Human Neutrophil Granulocytes From Patients With Monogenic Disease Using Data-independent Acquisition. *Mol. Cell. Proteomics* **18**, 760-772 (2019).
80. Doornebal, C.W.*, et al.* A preclinical mouse model of invasive lobular breast cancer metastasis. *Cancer Res.* **73**, 353-363 (2013).
81. Cox, J.*, et al.* Accurate proteome-wide label-free quantification by delayed normalization and maximal peptide ratio extraction, termed MaxLFQ. *Mol. Cell. Proteomics* **13**, 2513-2526 (2014).
82. Tyanova, S.*, et al.* The Perseus computational platform for comprehensive analysis of (prote) omics data. *Nat. Methods* **13**, 731-740 (2016).
83. Ashburner, M.*, et al.* Gene ontology: tool for the unification of biology. The Gene Ontology Consortium. *Nat. Genet.* **25**, 25-29 (2000).
84. The Gene Ontology, C. The Gene Ontology Resource: 20 years and still GOing strong. *Nucleic Acids Res.* **47**, D330-D338 (2019).